

# Relative Ordering and Spacing of $n$ and $\pi$ Levels in Isomeric Bipyrimidines. A Theoretical and Gas-Phase UV Photoelectron Spectroscopic Study

Vincenzo Barone,<sup>\*1a</sup> Carla Cauletti,<sup>1b</sup> Francesco Leij,<sup>\*1a</sup> Maria Novella Piancastelli,<sup>1b</sup> and Nino Russo<sup>1c</sup>

Contribution from the Istituto Chimico, Università di Napoli, I-80134 Napoli, Italy, Istituto di Chimica Generale ed Inorganica, Università di Roma, I-00100 Roma, Italy, and Dipartimento di Chimica, Università della Calabria, I-87030 Arcavacata di Rende (CS), Italy.

Received October 5, 1981

**Abstract:** The gas-phase UV photoelectron spectra of four isomeric bipyrimidines have been measured by using both He I and He II radiation. Theoretical computations by semiempirical and ab initio methods have been performed to better analyze the relative ordering of  $n$  and  $\pi$  energy levels. Koopmans' approximation is in general not adequate to reproduce the correct sequence of ionic states. On the other hand, the HAM/3 method gives results in much better agreement with experimental findings. The trend of ionic states in going from pyrimidine to different bipyrimidines has been carefully investigated. The use of well-chosen fragments and reference levels has allowed the development of a simple model able to interpret the PE spectra. On these grounds, simple rules of thumb that may prove useful in classifying the relevance of different interactions in determining the modifications of ionic states have been suggested.

The interpretation of gas-phase UV photoelectron spectra (PES) of azabenzene has stimulated considerable interest and is the subject of a number of experimental<sup>2-10</sup> and theoretical<sup>3,5-7,11-20</sup> investigations. The assignment of the PE spectra caused severe problems, and quite divergent interpretations have been given. In particular, Koopmans' approximation, which proved quite successful in most cases (see, for instance, ref 21 and 22 for a discussion and references), seems inadequate to reproduce the

correct relative ordering and spacing of ionic states in azabenzene.<sup>18</sup> This has not been ascribed to basis-set deficiency but rather to very nonuniform many-body effects, which strongly shift (to lower values) the ionization energies of  $n$  electrons with respect to those of  $\pi$  electrons.<sup>18,23-25</sup>

PE spectra<sup>26,27</sup> and theoretical computations<sup>26-34</sup> have also been reported for several polypyridines. On the other hand, bipyrimidines have not been investigated in the same detail<sup>35</sup> notwithstanding their potential interest as effective chelating agents. It was, therefore, interesting to record and analyze (with the aid of reliable quantum-chemical methods) the PE spectra of all the bipyrimidines synthesized until now<sup>36,37</sup> and reported in Figure 1.

The aim of this study is to test the possibility of interpreting the PE spectral patterns of large molecules by means of widely used quantum-chemical algorithms at both semiempirical and nonempirical single-determinant levels. This involves a careful comparison between experimental data and several theoretical computations concerning absolute values, relative ordering, and general trends of ionic states within a class of closely related molecules. The choice of the class of molecules is critical because it should allow the selection of only a limited number of predominant effects. Bipyrimidines fulfill this condition since the difference among the ionic states of the various isomers depends only on the different connectivities between identical subunits. This allows a clear-cut analysis of the trends within the whole class of molecules starting with the single subunit (in the present case pyrimidine) as a reference molecule.

(1) (a) Università di Napoli. (b) Università di Roma. (c) Università della Calabria.

- (2) Yench, A. J.; El-Sayed, M. A. *J. Chem. Phys.* **1968**, *48*, 3469.
- (3) Dewar, M. J. S.; Worley, S. D. *J. Chem. Phys.* **1969**, *51*, 236.
- (4) Turner, D. W.; Baker, C.; Baker, A. D.; Brundle, C. R. "Molecular Photoelectron Spectroscopy"; Wiley: London, 1970.
- (5) Jonsson, B. O.; Lindholm, E.; Skeberle, A. *Int. J. Mass Spectrom. Ion Phys.* **1969**, *3*, 385.
- (6) Fridh, C.; Asbrink, L.; Jonsson, B. O.; Lindholm, E. *Int. J. Mass Spectrom. Ion Phys.* **1972**, *8*, 85-101, 215-229, **1972**, *9*, 485.
- (7) Gleiter, R.; Heilbronner, E.; Horung, V. *Angew. Chem.* **1970**, *82*, 878; *Angew. Chem., Int. Ed. Engl.* **1970**, *9*, 910; *Helv. Chim. Acta* **1970**, *55*, 255.
- (8) Batick, C.; Heilbronner, E.; Horning, V.; Ashe, III, A. J.; Clark, D. T.; Coble, U. T.; Kilcast, D.; Scnalau, I. *J. Am. Chem. Soc.* **1973**, *95*, 928.
- (9) Heilbronner, E.; Maier, J. P.; Haselbach, E. *Phys. Methods Heterocycl. Chem.* **1974**, *6*, 1.
- (10) Heilbronner, E.; Horning, V.; Bock, H.; Alt, H. *Angew. Chem.* **1969**, *81*, 537; *Angew. Chem., Int. Ed. Engl.* **1969**, *8*, 524.
- (11) Ellis, R. L.; Jaffe, H. H.; Masmanidis, C. A. *J. Am. Chem. Soc.* **1974**, *96*, 2623.
- (12) Petke, J. D.; Whitten, J. W.; Ryan, J. A. *J. Chem. Phys.* **1968**, *48*, 953.
- (13) Clementi, E. *J. Chem. Phys.* **1967**, *46*, 4731; **1967**, *47*, 4485.
- (14) Almlöf, J.; Roos, B.; Wahlgren, U.; Johansen, H. *J. Electron Spectrosc. Relat. Phenom.* **1973**, *2*, 51.
- (15) Spanget-Larsen, J. *J. Electron Spectrosc. Relat. Phenom.* **1973**, *2*, 33; **1974**, *3*, 369.
- (16) (a) Wadt, W. R.; Goddard, W. A., III *J. Am. Chem. Soc.* **1975**, *97*, 2034. (b) Wadt, W. R.; Goddard, W. A., III; Dunning, T. H. *J. Chem. Phys.* **1976**, *65*, 438.
- (17) von Niessen, W.; Diercksen, G. H. F.; Cederbaum, L. S. *Chem. Phys.* **1975**, *10*, 345.
- (18) von Niessen, W.; Kraemer, W. P.; Diercksen, G. H. F. *Chem. Phys.* **1979**, *41*, 113.
- (19) Dewar, M. J. S.; Yamaguchi, Y.; Doraiswamy, S.; Sharma, S. D.; Suck, S. H. *Chem. Phys.* **1979**, *41*, 21.
- (20) Del Bene, J. E. *J. Am. Chem. Soc.* **1979**, *101*, 6184.
- (21) von Niessen, W.; Cederbaum, L. S.; Diercksen, G. H. F. *J. Chem. Phys.* **1977**, *67*, 4124.
- (22) von Niessen, W.; Cederbaum, L. S.; Domcke, W. NATO Advanced Study Institute: "Excited States in Quantum Chemistry"; Nicolaides, C. A. Beck, D. R. Eds.; Reidel: Dordrecht, 1978; pp 183-272.

- (23) Cederbaum, L. S. *Theor. Chim. Acta* **1973**, *31*, 239; *J. Phys. B.* **1975**, *8*, 290.
- (24) Cederbaum, L. S.; Domcke, W. *Adv. Chem. Phys.* **1977**, *36*, 205.
- (25) Schirmer, J.; Cederbaum, L. S. *J. Phys. B.* **1978**, *11*, 1889.
- (26) Maier, J. P.; Turner, D. W. *Faraday Discuss. Chem. Soc.* **1972**, *54*, 149.
- (27) Novak, I.; Klasinc, L. *Z. Naturforsch. A.* **1978**, *33A*, 247.
- (28) Favini, G. *Gazz. Chim. Ital.* **1964**, *94*, 1287.
- (29) Hofmann, H. J. *Z. Chem.* **1975**, *15*, 76.
- (30) Galasso, V.; De Alti, G.; Bigotto, A. *Tetrahedron* **1971**, *27*, 991.
- (31) Bossa, M.; Ramunni, G.; Franchini, D. F. *Theor. Chim. Acta* **1970**, *17*, 327.
- (32) Borgen, O.; Mestvedt, B.; Skanvik, I. *Acta Chem. Scand., Ser. A* **1976**, *30*, 43.
- (33) Benedix, R.; Birner, P.; Birnstock, F.; Hennig, H.; Hofmann, H. *J. Mol. Struct.* **1979**, *51*, 99.
- (34) Barone, V.; Cristinziano, P. L.; Leij, F.; Russo, N., *Gazz. Chim. Ital.*, in press.
- (35) (a) Leij, F.; Russo, N.; Chidichimo, G. *Chem. Phys. Lett.* **1980**, *69*, 530. (b) Fernholt, L.; Romming, C.; Samdal, S. *Acta Chem. Scand., Ser. A* **1981**, *A35*, 707.
- (36) Musgrave, F. R.; Westcott, P. A. *Org. Synth.* **1972**, *52*, 1799.
- (37) Kauffmann, T. *Angew. Chem., Int. Ed. Engl.* **1979**, *18*, 1.

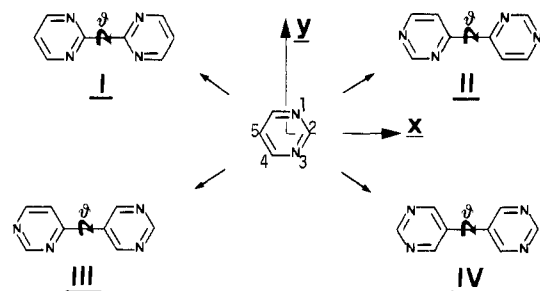


**Figure 1.** Molecular structure and labeling of bipyrimidines. The adopted reference frame is also shown. The reported conformations correspond to a  $\varphi$  dihedral angle of  $0^\circ$ .

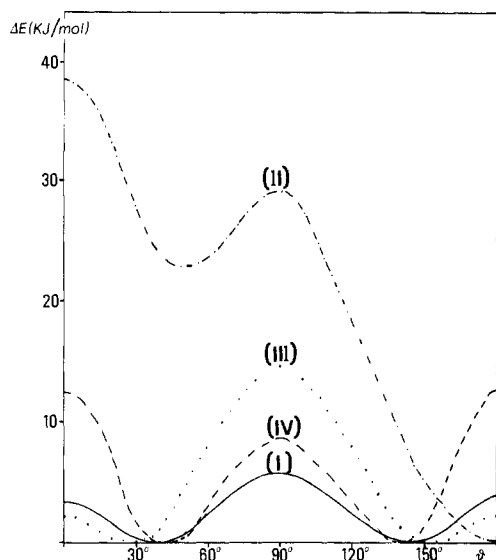


**Figure 2.** Torsional curves of the different bipyrimidines according to STO-3G computations (ref 51b).

On these grounds, an attempt is made to develop a simple model able to formalize and evaluate the relative weight of different interactions.

### Experimental Section

The compounds were synthesized as described in ref 36 for 2,2'-bipyrimidine (I) and in ref 37 for the other three molecules.

He I and He II photoelectron spectra were run on a Perkin-Elmer PS18 instrument equipped with a dual He I/He II source (Helectros Development) at temperatures between 76 and 116 °C. Ar, CH<sub>3</sub>I, and self-ionizing He were used as internal standards.

### Quantum-Chemical Computations

Ionization energies have been computed by IEHT,<sup>38,39</sup> INDO,<sup>40,41</sup> MNDO,<sup>42,43</sup> and ab initio (internal STO-3G basis set<sup>44</sup> of the GAUSSIAN/70 package<sup>45</sup>) methods using Koopmans' approximation and by the HAM/3 method<sup>46-48</sup> using the transition-state

(38) Hoffmann, R. *J. Chem. Phys.* **1963**, *39*, 1397.

(39) Program No. 358, Quantum Chemistry Program Exchange, Indiana University, Bloomington, IN.

(40) Pople, J. A.; Beveridge, D. L. "Approximate Molecular Orbital Theory"; McGraw-Hill: New York, 1970.

(41) Program No. 281, Quantum Chemistry Program Exchange, Indiana University, Bloomington, IN.

(42) Dewar, M. J. S.; Thiel, W. *J. Am. Chem. Soc.* **1977**, *99*, 4899, 4907.

(43) Program No. 353, Quantum Chemistry Program Exchange, Indiana University, Bloomington, IN.

(44) Hehre, W. J.; Stewart, R. F.; Pople, J. A. *J. Chem. Phys.* **1969**, *51*, 2657.

(45) Program No. 236, Quantum Chemistry Program Exchange, Indiana University, Bloomington, IN.

(46) Asbrink, L.; Fridh, C.; Lindholm, E. *Chem. Phys. Lett.* **1977**, *52*, 63, 69, 72.

(47) Asbrink, L.; Fridh, C.; Lindholm, E. De Bruijn, S.; Chong, D. P. *Phys. Scr.* **1980**, *22*, 475.

(48) Program No. 393, Quantum Chemistry Program Exchange, Indiana University, Bloomington, IN.

**Table I.** Composition of the Highest Four MO's of Pyrimidine<sup>a</sup>

		$\pi$ Orbitals			
		$a_2 (\pi_2)$		$b_1 (\pi_3)$	
atom	orbital	STO-3G	HAM/3	STO-3G	HAM/3
N1	2p <sub>z</sub>	0.489	0.530	0.248	0.250
C2	2p <sub>z</sub>			0.491	0.440
C4	2p <sub>z</sub>	-0.433	-0.411	-0.289	-0.314
C5	2p <sub>z</sub>			-0.568	-0.591
		$\eta$ Orbitals			
		$a_1 (n_g)$		$b_2 (n_A)$	
atom	orbital	STO-3G	HAM/3	STO-3G	HAM/3
N1	2s	0.386	0.276	-0.321	-0.213
	2p <sub>x</sub>	0.413	0.452	-0.219	-0.232
	2p <sub>y</sub>	0.245	0.312	-0.537	-0.566
C2	2s	0.166	0.159		
	2p <sub>x</sub>				
	2p <sub>y</sub>			0.236	0.163
C4	2s				
	2p <sub>x</sub>	-0.240	-0.195		
	2p <sub>y</sub>			0.116	0.120
C5	2s	-0.116	-0.083		
	2p <sub>x</sub>	0.229	0.216		
	2p <sub>y</sub>			-0.258	-0.248
H(C2)	1s	0.273	0.156		
H(C4)	1s			-0.161	-0.087
H(C5)	1s	-0.213	-0.111		

<sup>a</sup> The reference frame and the numbering of the atoms are the same as in Figure 1.

approximation<sup>49,50</sup> and removing the charge 0.5—uniformly from all the occupied valence orbitals ("diffuse ionization")<sup>46</sup> to analyze the merits and pitfalls of the most widely used quantum-chemical methods.

It has been previously shown (e.g., ref 18 and 51a) that the computed ionization energies may strongly depend on the molecular geometry, so that the knowledge of an accurate geometry of the studied molecules is a mandatory starting point. Due to the lack of experimental data, the chosen geometries are obtained from two pyrimidine rings optimized at the MNDO or STO-3G (also used for IEHT, INDO, and HAM/3 computations) level with an inter-ring distance (1.50 Å) evaluated in an electron diffraction study of 2,2'-bipyrimidine.<sup>35</sup> Further details are given in ref 51b. As for molecular conformations, Figure 2 summarizes the results obtained in a previous study using STO-3G computations.<sup>51b</sup> It can be seen that I, III, and IV have a nonplanar equilibrium conformation. However, the computed torsional barriers do not exclude a significant contribution, under measurement conditions, of planar structures. On the contrary, a planar equilibrium conformation is predicted for II, and the computed torsional energy barriers are large enough to prevent a significant deviation from planarity, even under experimental conditions.

On the grounds of the above considerations, we have computed the ionization energies of the different bipyrimidines for both planar and equilibrium conformations.

### Results and Discussion

**I. Pyrimidine as a Reference Fragment.** For a better understanding of the features of the PE spectra of bipyrimidines, it is useful to refer to the energy level and MO composition of the parent molecule pyrimidine.

We shall be mainly concerned with the highest occupied (four n type and four  $\pi$  type) orbitals of bipyrimidines. These are essentially derived from the pairs 5b<sub>2</sub>, 7a<sub>1</sub> (n type) and 2b<sub>1</sub>, 1a<sub>2</sub> ( $\pi$  type) of pyrimidine. The composition of these MO's according

(49) Slater, J. C. *Adv. Quantum Chem.* **1972**, *6*, 1.

(50) Brandi, H. S.; De Matos, M. M.; Ferreira, R. *Chem. Phys. Lett.* **1980**, *73*, 597.

(51) (a) Barone, V.; Bucci, P.; Leij, F.; Russo, N. *J. Mol. Struct.* **1981**, *76*, 29. (b) Barone, V.; Cristinziano, P. L.; Leij, F.; Russo, N., submitted for publication.

Table II. Ionic States of Pyrimidine ( $C_{2v}$  Point Group) According to Different Methods

symmetry		exptl <sup>b</sup>	HAM/3 <sup>c</sup>	STO-3G <sup>c</sup>	MNDO <sup>d,e</sup>	HF-2 $\zeta$ <sup>f,g</sup>	GF <sup>f,g</sup>	TDA <sup>f,g</sup>
$C_{2v}$	$C_s^a$							
5b <sub>2</sub>	n <sub>A</sub>	9.7	10.00	9.38	10.82	11.43	9.50	9.86
2b <sub>1</sub>	$\pi_3$	10.5	10.70	8.98	10.38	10.83	10.54	10.43
7a <sub>1</sub>	n <sub>S</sub>	11.2	11.04	10.81	12.44	12.79	10.87	11.15
1a <sub>2</sub>	$\pi_2$	11.5	11.39	9.67	11.53	11.74	11.23	11.16
2a <sub>2</sub> <sup>h</sup>	$\pi^*$		0.00	-5.75	0.17	-2.11		
3b <sub>1</sub> <sup>h</sup>	$\pi^*$		-0.56	-6.21	0.30	-2.62		

<sup>a</sup> We use the labels n and  $\pi$  in place of the usual a' and a''. <sup>b</sup> Quoted in ref 18. <sup>c</sup> STO-3G-optimized geometry. <sup>d</sup> MNDO-optimized geometry. <sup>e</sup> Reference 19. <sup>f</sup> X-ray geometry. <sup>g</sup> Reference 18. <sup>h</sup> Electron affinities for empty orbitals; they are computed by using Koopman's approximation for ab initio and MNDO methods and by adding a  $-1/2$  charge uniformly to all the valence empty orbitals in the case of the HAM/3 method.

to STO-3G and HAM/3 methods is reported in Table I. It can be seen that the agreement between the two methods is generally good, even if some discrepancies exist that can have relevant consequences (see part III of this section).

The experimental ordering of ionization energies (IE's) of pyrimidine is  $5b_2 < 2b_1 < 7a_1 < 1a_2$  (Table II). Only the Green function techniques and the HAM/3 method satisfactorily reproduce the ordering of ionic states and the IE's. On the other hand, the STO-3G and MNDO methods parallel the ordering of the extended basis-set ab initio computations. In particular, the MNDO results are in remarkable quantitative agreement with previous good quality, nonempirical computations.

The pyrimidine molecule possesses  $\sigma$ ,  $\pi$  separability and low-lying  $\pi^*$  MO's (Table II). Hence, as previously shown,<sup>52-54</sup> the n( $\sigma$ ) occupied MO's are likely to undergo large many-body corrections that alter the ordering of ionic states provided by Koopmans' approximation. The same applies to bipyrimidines, in which low-lying  $\pi^*$  MO's exist at energies even lower than those in pyrimidine. The resulting many-body effects can be accounted for by Green function<sup>18,54</sup> or perturbative<sup>52,53,55</sup> formalisms, but these techniques are out of the question in the present case due to the large dimensions of bipyrimidines. Also, ab initio computations employing extended basis sets (which would be mandatory to reproduce quantitatively IE's, at least when Koopmans' approximation holds) are hardly feasible in this context. Furthermore, they could provide only a reference ordering of ionic states, which may be useful in estimating the relevance of correlation and relaxation effects. Anyway, this qualitative role can be fulfilled as well by less expensive STO-3G and MNDO computations.

On the other hand, the very good results obtained by the HAM/3 method for several azabenzenes<sup>18</sup> and 2,2'-bipyridine<sup>34</sup> allow us to be quite confident about the use of this method for the interpretation of the PE spectra of bipyrimidines.

In going from pyrimidine to different bipyrimidines, we expect the doubling of each level of pyrimidine to happen, mainly due to its symmetric or antisymmetric combination with the corresponding level of the second pyrimidine ring. The similar origin of corresponding ionic states in bipyrimidines belonging to different point groups is better evidenced by using the nomenclature shown in Scheme I.

**II. Assignment of Spectra of Bipyrimidines.** Spectral patterns of the four isomeric bipyrimidines are quite interesting due to their remarkable differences. This behavior, which is not obvious in such a series of similar molecules, indicates a significant variation in both kind and magnitude of interactions between the two conjugated rings, strongly dependent on the relative position of nitrogen atoms.

He I spectra are reported in Figure 3; we also recorded the He II spectra, but they do not show any appreciable variation in

Scheme I

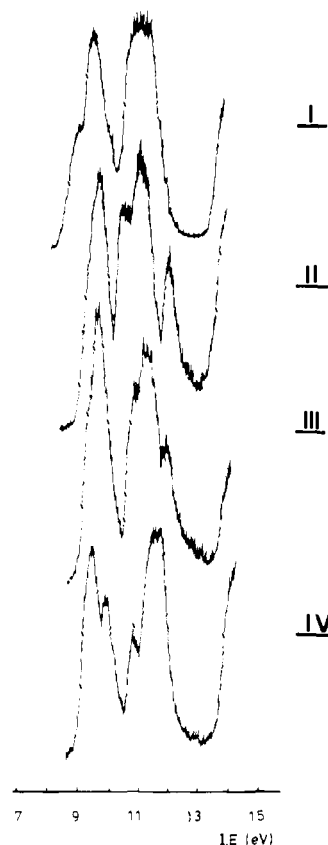
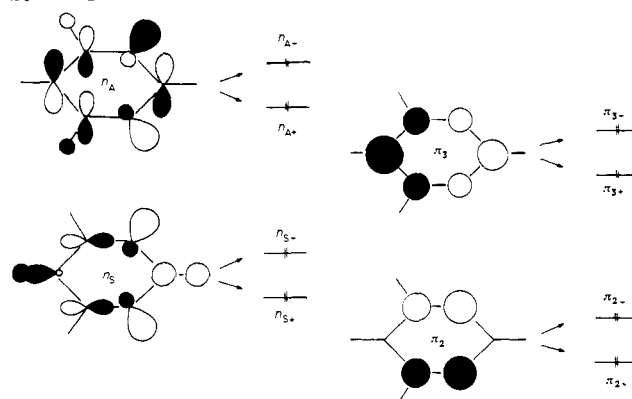


Figure 3. He I PE spectra of bipyrimidines; the molecules are labeled as in Figure 1.

relative cross sections and are, therefore, of no help in the assignment of peaks.

The analysis of the experimental PES data is not trivial in all cases, due to the complexity of the molecules and, in particular, to the presence of many ionic states in the same energy region,

(52) Chong, D. P.; Herring, F. G.; McWilliams, D. J. *Electron Spectrosc. Relat. Phenom.* **1975**, *7*, 445.

(53) Chong, D. P.; Herring, F. G.; Takahata, Y. *J. Electron Spectrosc. Relat. Phenom.* **1978**, *13*, 39.

(54) Cederbaum, L. S. *Chem. Phys. Lett.* **1974**, *25*, 562.

(55) Chong, D. P.; Herring, F. G.; McWilliams, D. J. *J. Chem. Phys.* **1974**, *61*, 78, 958, 3567.

Table III. Ionic States of 2,2'-Bipyrimidine (I) at Both Its Equilibrium ( $D_2$  Symmetry,  $\vartheta = 40^\circ$ ) and Planar ( $D_{2h}$  Symmetry) Conformations<sup>a</sup>

symmetry					exptl	HAM/3 <sup>b</sup>	HAM/3 <sup>c</sup>	STO-3G <sup>b</sup>	STO-3G <sup>d</sup>	STO-3G <sup>e</sup>	MNDO <sup>e</sup>	MNDO <sup>f</sup>	INDO <sup>b</sup>	IEHT <sup>b</sup>
$D_{2h}$	$D_2$	$C_{2h}$	$C_{2v}$	$C_s^g$										
$b_{1g}$	$b_1$	$a_g$	$b_2$	$n_{A^-}$	9.17	9.24	9.23	8.79	8.68	9.07	10.58	10.84	10.75	11.69
$b_{2u}$	$b_2$	$b_u$	$b_2$	$n_{A^+}$	9.59	9.35	9.24	9.46	9.37	9.35	10.74	11.07	11.39	12.03
$b_{2g}$	$b_2$	$b_g$	$b_1$	$\pi_{3^-}$										
$a_g$	$a$	$a_g$	$a_1$	$n_{S^+}$	10.82	10.36	10.23	10.40	10.46	10.22	12.18	12.22	11.57	12.37
$b_{1u}$	$b_1$	$a_u$	$b_1$	$\pi_{3^+}$										
$a_u$	$a$	$a_u$	$a_2$	$\pi_{2^-}$	11.21	10.63	10.70	9.44	9.69	9.51	11.42	11.46	14.31	14.00
$b_{3u}$	$b_3$	$b_u$	$a_1$	$n_{S^-}$										
$b_{3g}$	$b_3$	$b_g$	$a_2$	$\pi_{2^+}$	10.70	10.73	9.54	9.82	9.48	11.42	11.51	14.46	13.96	

<sup>a</sup> The MO's are classified for the  $D_{2h}$  group and for all its subgroups relevant for the other bipyrimidines. The reference axes are oriented as shown in Figure 1. <sup>b</sup> Planar conformation; STO-3G geometry with an inter-ring distance of 1.50 Å. <sup>c</sup> Equilibrium conformation; STO-3G geometry with an inter-ring distance of 1.50 Å. <sup>d</sup> Planar conformation; X-ray geometry for the pyrimidine rings and inter-ring distance of 1.50 Å. <sup>e</sup> Planar conformation; MNDO geometry with an inter-ring distance of 1.50 Å. <sup>f</sup> Equilibrium conformation; MNDO geometry with an inter-ring distance of 1.50 Å. <sup>g</sup> We use the labels  $n$  and  $\pi$  in place of  $a'$  and  $a''$  to better visualize the origins of the different MO's.

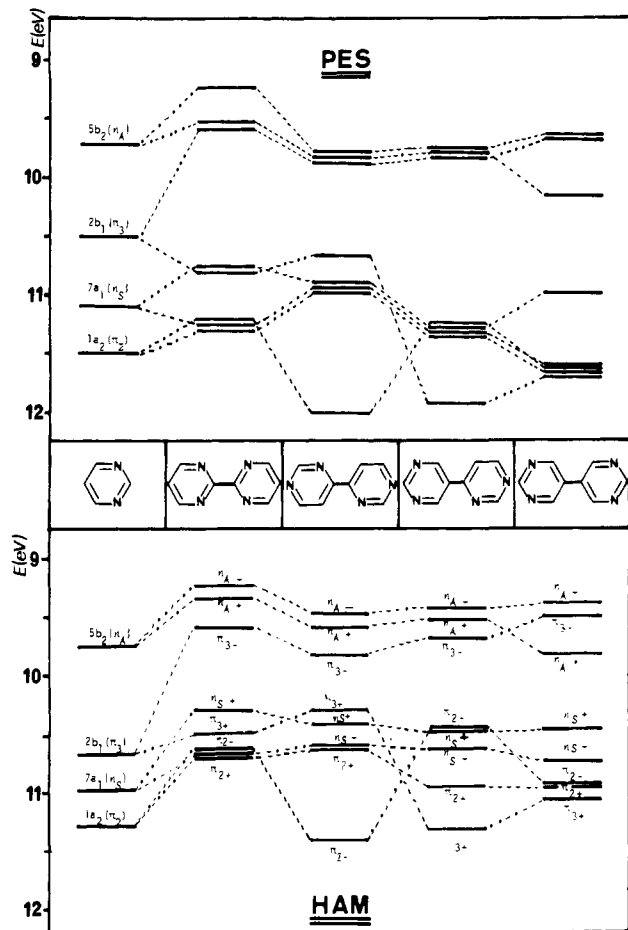


Figure 4. Comparison between experimental and HAM/3 ionization energies for pyrimidine and isomeric bipyrimidines.

giving rise to composite bands. In such a situation, calculated IE's close to the experimental ones and with a good internal coherence (in what concerns the relative position of energy levels) are needed to succeed in interpreting PE spectra. Among the various computational methods used (see the next section), HAM/3 proved to be very satisfactory with respect to the absolute energy values (Figure 4); furthermore, the sequence of ionic states and the MO compositions obtained by this method are consistent with spectral trends along the whole series. Our assignment is therefore based essentially on the HAM/3 data; considerations based on the relative band areas are used to support the analysis but not as main criterion, due to the different cross sections of carbon and nitrogen atomic orbitals and the complexity of band envelopes.

The spectrum of 2,2'-bipyrimidine (I) exhibits two composite bands in the energy region between 9 and 12 eV (Figure 3), with

Table IV. Ionic States of 4,4'-Bipyrimidine (II) in Its Equilibrium ( $C_{2h}$ ) Conformation<sup>a</sup>

symmetry		exptl	HAM/3 <sup>b</sup>	STO-3G <sup>b</sup>	MNDO <sup>c</sup>	INDO <sup>b</sup>	IEHT <sup>b</sup>
$C_{2h}$	$C_s^g$						
$a_g$	$n_{A^-}$	9.86	9.48	9.40	10.88	10.63	11.70
$b_u$	$n_{A^+}$						
$b_g$	$\pi_{3^-}$	10.65	9.84	8.34	10.12	12.47	13.24
$a_u$	$\pi_{3^+}$						
$a_g$	$n_{S^+}$	10.90	10.39	10.72	12.39	12.26	12.28
$b_u$	$n_{S^-}$						
$b_g$	$\pi_{2^+}$	12.00	10.64	9.50	11.36	14.32	13.77
$a_u$	$\pi_{2^-}$						

<sup>a</sup> The meaning of the superscripts is the same as in Table III.

an intensity ratio of  $\sim 3:5$ . The first band has a shoulder at 9.17 eV and a maximum at 9.59 eV; in the second broad band we identify two maxima at 10.82 and 11.21 eV.

Computations performed by HAM/3 and STO-3G methods (Table III) at different conformations show that the effect of the deviation from planarity on the orbital energy values is quite low; therefore, in this context we can confidently use the planar conformation levels, which retain  $\sigma$ ,  $\pi$  separability.

By analogy with the azabenzenes series,<sup>18</sup> we also expect in this case an n-type level to be ionized first. Therefore, we can assign the shoulder at 9.17 eV to the ionization of the first combination of the two  $b_2$  levels of pyrimidine rings; the band at 9.59 eV accounts for the ionization of the second combination of the same levels plus the first  $\pi$ -type level. The second broad band arises from the ionization of the remaining five (three  $\pi$  type and two n type) levels.

The absolute HAM/3 values and the spacings match the experimental findings quite well. As for n levels, the antisymmetric combination  $n_{A^-}$  is less stable than the symmetric one,  $n_{A^+}$ , but the opposite occurs for the second pair of levels; i.e.,  $n_{S^+}$  is less stable than  $n_{S^-}$ . In fact, in the first pair of levels, both the interactions between nitrogen lone pairs and between the  $\sigma$  orbitals of inter-ring carbon atoms ( $C_{ir}$ ) are destabilizing in  $n_{A^-}$  and stabilizing in  $n_{A^+}$  orbitals (Scheme I), with coefficients similar in magnitude in both cases; this effect accounts for the relative position of these levels. The same applies to the second pair of n orbitals ( $n_{S^+}$  and  $n_{S^-}$ ), but in this case the relative weight of  $C_{ir}$  atoms with respect to nitrogen atoms is higher in  $n_{S^+}$  than in  $n_{S^-}$ , so that the  $n_{S^-}$  level is lowered in energy by the effect of the higher electronegativity of nitrogen.

As for the  $\pi$ -type orbitals, (Figure 5), the highest two levels are the antisymmetric and symmetric combinations of the  $\pi_3$  levels of the two pyrimidine rings. The splitting between these orbitals is relevant and is essentially due to the bonding or antibonding interaction between  $C_{ir}$  atoms. The second two  $\pi$ -type levels ( $\pi_{2^-}$  and  $\pi_{2^+}$ ) are nearly degenerate because the contribution of  $C_{ir}$  atoms is zero by symmetry (Figure 5) and the conjugation between the two rings is not appreciable.

The spectrum of 4,4'-bipyrimidine (II) is more articulated than that of I (Figure 3). In the low-energy region it shows four bands

Table V. Ionic States of 4,5'-Bipyrimidine (III) both at Equilibrium ( $\vartheta = 28^\circ$ ) and Planar Conformations<sup>a</sup>

symmetry, $C_s^g$	energy (eV)					
	exptl	HAM/3	STO-3G <sup>b</sup>	MNDO <sup>e</sup>	INDO <sup>b</sup>	HAM/3 <sup>c</sup>
$n_{A^-}$	9.77	9.47	9.46	10.83	10.98	9.45
$n_{A^+}$		9.56	9.67	11.03	11.48	9.53
$\pi_{3^-}$	11.28	9.73	8.20	9.90	12.17	9.84
$\pi_{2^-}$		10.45	9.48	10.88	14.21	10.48
$n_{S^+}$	11.28	10.50	11.02	12.56	12.68	10.49
$n_{S^-}$		10.65	11.10	12.63	12.94	10.63
$\pi_{2^+}$	11.91	10.95	9.86	11.66	14.66	10.97
$\pi_{3^+}$		11.34	10.72	12.06	16.30	11.29

<sup>a</sup> The meaning of the superscripts is the same as in Table III.

with intensity ratios of ca. 3:1:3:1 and maxima at 9.86, 10.65, 10.90, and 12.00 eV. The proposed assignment is the following (Table IV): The first triple band is related to the ionization of the first pair of n-type levels ( $n_{A^-}$  and  $n_{A^+}$ ) and one  $\pi$ -type level; the second single band arises from the ionization of the second  $\pi$ -type level; the third triple band accounts for the ionization of the second pair of n-type levels ( $n_{S^+}$  and  $n_{S^-}$ ) and the third  $\pi$ -type level; finally, the fourth single band arises from the ionization of the fourth  $\pi$ -type level.

As for the n-type orbitals, their relative ordering is determined by factors analogous to those found in I; however, in II, nitrogen atoms are far from each other, and the contribution of  $C_{ir}$  atoms is always small. As a consequence, the splitting within each pair of levels is reduced, and, in particular, the two highest n-type orbitals are nearly degenerate. As for the  $\pi$ -type levels (Figure 5), there is a noticeable difference with respect to I concerning both relative ordering and splittings. The main variation is that in II the  $\pi_{2^-}$  orbital is greatly stabilized with respect to the analogous level in I. This effect (confirmed by all the quantum-chemical methods used) can be explained by observing the composition of the  $\pi_{2^-}$  orbital in I and II. The coefficients of  $C_{ir}$  atoms are quite large and of the same sign in II, while the corresponding  $\pi$ -type level in I does not receive any contribution from  $C_{ir}$  orbitals for symmetry reasons (Figure 5).

The spectrum of 4,5'-bipyrimidine (III) (Figure 3) is quite similar to that of II: it exhibits three bands with intensity ratios of 3:4:1 and maxima at 9.77, 11.28, and 11.91 eV (the second band has a shoulder at ca. 10.90 eV). The assignment (Table V) is completely analogous to that of II, and the first band accounts for the ionization of two n-type and one  $\pi$ -type levels, the second band arises from the ionization of two n-type and two  $\pi$ -type levels, and the third band corresponds to the fourth  $\pi$ -type level. The relative ordering of levels and the molecular orbital compositions (Figures 4 and 5) are intermediate between those of II and IV, with the obvious differences due to the lower symmetry.

The spectrum of 5,5'-bipyrimidine (IV) is quite different with respect to all the other cases (Figure 3). It shows four bands with intensity ratios of ca. 2:1:1:4 and maxima at 9.68, 10.13, 10.94, and 11.62 eV. As already found for I, both HAM/3 and STO-3G computations performed at a planar conformation or at  $\vartheta = 43^\circ$  (equilibrium conformation according to STO-3G computations<sup>51</sup>)

Table VI. Ionic States of 5,5'-Bipyrimidine (IV) Both at Its Equilibrium ( $D_2$  Symmetry,  $\vartheta = 42^\circ$ ) and Planar ( $D_{2h}$  Symmetry) Conformations<sup>a</sup>

symmetry		energy (eV)													
$D_{2h}$	$D_2$	$C_{2h}$	$C_{2v}$	$C_s^g$	exptl	HAM/3 <sup>b</sup>	HAM/3 <sup>c</sup>	STO-3G <sup>b</sup>	STO-3G <sup>d</sup>	STO-3G <sup>c</sup>	MNDO <sup>e</sup>	MNDO <sup>f</sup>	INDO <sup>b</sup>	IEHT <sup>b</sup>	
$b_{1g}$	$b_1$	$a_g$	$b_2$	$n_{A^-}$	9.68	9.39	9.39	9.43	9.48	9.45	10.93	10.91	10.91	11.53	
$b_{2g}$	$b_2$	$b_g$	$b_1$	$\pi_{3^-}$		9.57	9.52	8.03	8.44	8.17	9.80	9.87	11.85	13.04	
$b_{2u}$	$b_2$	$b_u$	$b_1$	$n_{A^+}$	10.13	9.66	9.86	9.96	10.04	9.92	11.25	11.24	12.06	12.14	
$a_g$	$a$	$a_g$	$a_1$	$n_{S^+}$	10.94	10.53	10.51	10.65	10.78	10.64	12.43	12.43	12.06	12.24	
$b_{3u}$	$b_3$	$b_u$	$a_1$	$n_{S^-}$	11.62	10.79	10.78	11.68	11.68	11.68	13.37	13.36	13.33	12.67	
$a_u$	$a$	$a_u$	$a_2$	$\pi_{2^-}$		10.91	10.98	9.97	10.31	10.00	11.81	11.81	14.56	13.85	
$b_{3g}$	$b_3$	$b_g$	$a_2$	$\pi_{2^+}$	10.97	11.00	10.04	10.37	10.01	11.81	11.81	14.69	13.90		
$b_{1u}$	$b_1$	$a_u$	$b_1$	$\pi_{3^+}$	11.26	11.12	10.63	11.06	10.47	11.74	11.65	16.34	14.21		

<sup>a</sup> The meaning of the superscripts is the same as in Table III.

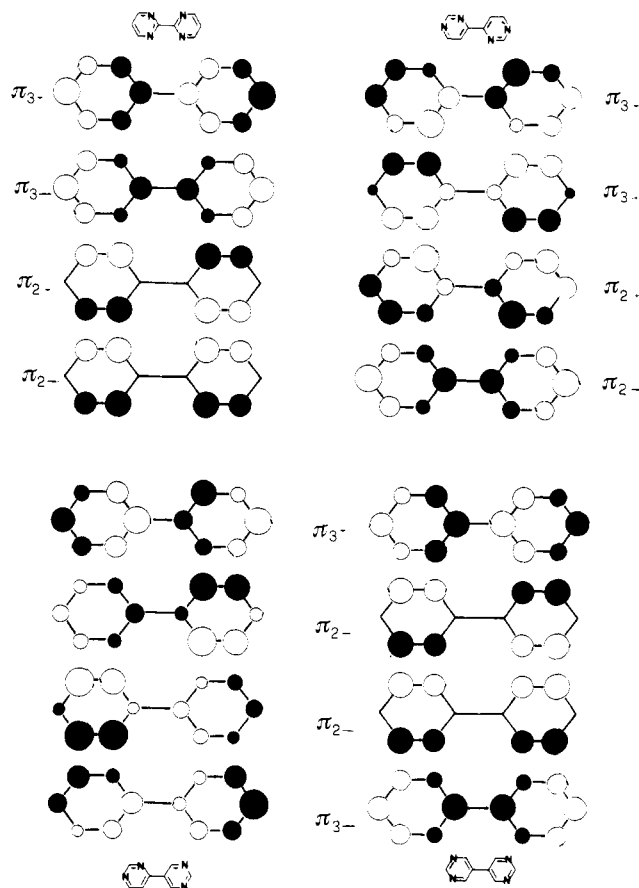


Figure 5. Schematic drawing of the  $\pi$  molecular orbitals for the studied bipyrimidines. The radii of the circles representing the different atomic orbitals are proportional to their coefficients in the MO's.

do not reveal significant variations (Table VI); therefore, we can consider the two rings coplanar in classifying levels as n or  $\pi$  type.

As for the assignment, the most interesting point is that HAM/3 calculations indicate a relevant splitting  $\Delta E$  between the highest two n-type levels and suggest that the first band accounts for the ionization of one n-type ( $b_{1g}$ ) and one  $\pi$ -type ( $b_{2g}$ ) level and the second band for the second n-type ( $b_{2u}$ ) level.

We point out that all the theoretical methods used agree in forecasting  $\Delta E$  larger (or very similar) for IV than for I. The experimental data fulfill this condition only by the above assignment ( $\Delta E \approx 0.42$  eV for I and 0.45 eV for IV). A rationalization of this effect by means of a simple two-orbital model will be given in part IV of this section.

The bands at 10.94 and 11.62 eV account for the other five orbitals and, on the basis of HAM/3 data, can be attributed to the third n-type ( $a_g$ ) level (third band) and the fourth n-type plus the three remaining  $\pi$ -type levels (fourth band). The relative ordering of n-type orbitals can be interpreted by means of considerations analogous to those used in the case of I, because the two molecules have the same symmetry. As for the  $\pi$ -type levels,

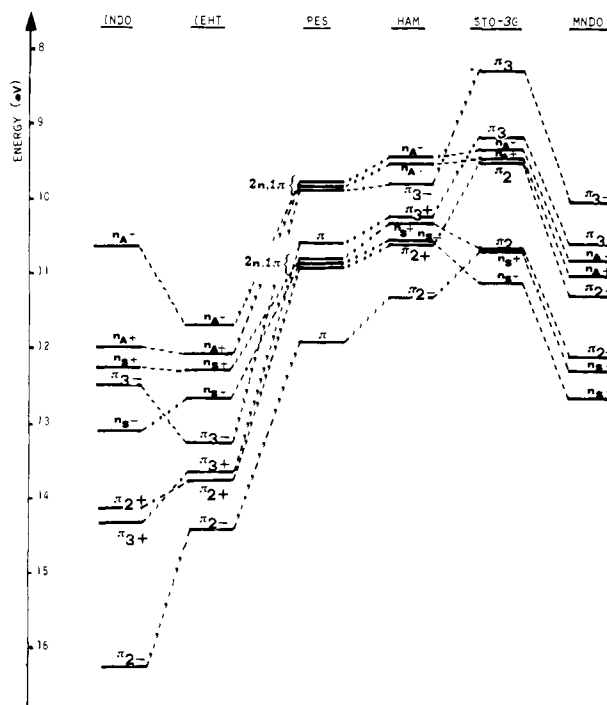


**Figure 6.** Comparison between experimental and theoretical (computed by several quantum-mechanical methods) ionization energies for 4,4'-bipyrimidine (II).

the situation of IV is quite similar to that of I with respect to the negligible splitting between  $\pi_{2+}$  and  $\pi_{2-}$  levels, but the  $\pi_{3+}$  level is greatly stabilized with respect to I.

### III. Comparison between Different Quantum-Chemical Methods.

There are two connections in which theoretical computations can be of help in the interpretation of PE spectra. The first is obviously the correct reproduction of the energies and relative ordering of ionic states. The second consists of the analysis of general trends and their interpretation in terms of (possibly) simple models.

As for the first point, only the HAM/3 method is able to reproduce (also quantitatively) the correct ordering of ionic states. This is shown in Tables III–VI and, in an impressive graphical form, in Figure 6. Figure 6 represents the ionic states obtained by several widely used quantum-chemical methods in the case of 4,4'-bipyrimidine (II). This molecule has been chosen as it does not involve any conformational problems (planar equilibrium conformation).

It can be seen that STO-3G and MNDO computations strongly destabilize  $\pi$  orbitals with respect to  $\sigma$  ones. This destabilization (eliminated by many-body effects, as previously discussed) is practically constant along the whole series of compounds. On the other hand, the relative ordering within each class of orbitals ( $n$  or  $\pi$ ) is in most cases correctly reproduced by both methods. As a matter of fact, linear relationships of the kind

$$IE_i(\text{exptl}) = -0.2 - \epsilon_i(\text{MNDO}) - \delta_{in}$$

$$\delta_{in} = 0 \text{ if } i \text{ is a } \pi \text{ orbital, } 1 \text{ if } i \text{ is an } n \text{ orbital}$$

or

$$IE_i(\text{exptl}) = 0.2 - \epsilon_i(\text{STO-3G}) + \delta_{i\pi}$$

$$\delta_{i\pi} = 0 \text{ if } i \text{ is an } n \text{ orbital, } 1 \text{ if } i \text{ is a } \pi \text{ orbital}$$

provide numerical results in close agreement with experimental results. This is due to the presence of low-lying  $\pi^*$  orbitals of about the same energy for all the studied compounds, which gives quasi-constant corrections to Koopmans' ionization energies.<sup>52,55</sup>

The INDO results are affected by a general over stabilization of ionic states together with the well-known over stabilization of  $\sigma$  orbitals with respect to  $\pi$  orbitals. Finally, the iterative EHT method always provides the same ordering of ionic states, with the four  $n$  levels being less stable than the four  $\pi$  levels in all the studied compounds.

Due to the very good performances of the HAM/3 method, it is perhaps interesting to point out some minor shortcomings. The results of the present study together with a comprehensive analysis of several other molecules suggest the following general considerations: (1) The stability of  $n$  states is slightly overestimated with respect to  $\pi$  states due to a general underestimation of conjugative effects. (2) The splitting between  $n$  levels is underestimated, this effect being particularly evident for the first pair of  $n$  levels in I.

More care must be devoted to the analysis and interpretation of general trends. To this end, we consider the variation of ionic states in going from pyrimidine (chosen as reference) to different bipyrimidines and consider separately  $n$  and  $\pi$  orbitals. In this connection, particular attention must be devoted to nonempirical results. It has been recently stated<sup>18</sup> that Koopmans' approximation, even if based on accurate ab initio computations, is useless in providing the correct ordering of ionic states in polyazabenzene. However, nonempirical computations allow an analysis of the different factors playing a role at the HF level clearer than semiempirical methods because in the former case no adjustable (and hence badly controllable) parameters are introduced. Although quantitative agreement with experimental data is not to be expected, a clear-cut analysis of general trends can be obtained in the present case since many-body corrections are likely to be nearly constant within each class ( $n$  or  $\pi$ ) of orbitals.

Figure 7A shows the variation of  $\pi$  levels in going from pyrimidine to the different bipyrimidines according to experimental and STO-3G results. Figure 7B shows the analogous trend for  $n$  orbitals.

As a first point, it can be observed that there is a remarkable agreement between the data from experiment and STO-3G calculations. As for  $\pi$  orbitals, consideration of nonplanar (equilibrium) conformations generally gives a better agreement with experimental data. The rationalization of the modifications of ionic levels upon torsion is trivial on inspection of the nodal characteristics of the pertinent MO's between the two rings; of course, bonding MO's are destabilized by torsion, and the opposite occurs for antibonding MO's, with the extent of the shift depending on the coefficients of  $C_{if}$  atoms. The situation is more intriguing for  $n$  orbitals. In particular, only the ab initio method provides (in agreement with experimental data) a similar splitting between  $n_{A+}$  and  $n_{A-}$  levels in I and IV. All the other methods suggest a much larger splitting between these two levels in IV. The reason can be found in the approximations introduced in the semiempirical methods, but another factor is the magnitude of the coefficients of carbon atoms in the  $n_A$  level of pyrimidine (Table I). In fact, while the STO-3G method gives coefficients similar for C2 and C5 (which become  $C_{if}$  atoms in I and IV, respectively) and much smaller for C4, all the other methods (as exemplified by HAM/3 in Table I) provide a much greater coefficient for the C5 atom. Conformational effects are significant for  $n$  levels only in I and are similar to those discussed for  $\pi$  levels.

The only serious discrepancy between STO-3G and experimental data concerns the pair  $n_{5-}$ ,  $n_{5-}$  of II, in which the theoretical splitting is much larger than the experimental one (this effect is common to all the quantum-chemical methods employed). This discrepancy cannot be ascribed to conformational effects because this molecule has a planar equilibrium conformation coupled to strong torsional barriers (Figure 2).

As a last point, we recall the need of employing a coherent molecular geometry when studying a class of related molecules; as shown in Tables III and VI, the use of different geometries can strongly alter the computed ionization energies.

Summarizing, we think that fragment analysis results in an extension of the range of applicability of Koopmans' approximation. In fact, separate consideration of  $n$  and  $\pi$  levels allows a detailed analysis of PE spectra in a class of closely related molecules whenever many-body corrections are nearly constant for each class of orbitals.

**IV. A Simple Two-Orbital Model.** We start from the MO's of the pyrimidine subunit (Table I) and make the simplifying hypothesis that each pair (symmetric  $\psi_i^+$  and antisymmetric  $\psi_i^-$

Table VII. Comparison between the Splittings Computed by the Simple Two-State Model ( $\Delta E^{\text{mod}}$ ) and Those Obtained by Complete Computations ( $\Delta E^{\text{calcd}}$ )<sup>a</sup>

	I			II			IV		
	$\pi_2$	$\pi_3$	$n_A$	$\pi_2$	$\pi_3$	$n_A$	$\pi_2$	$\pi_3$	$n_A$
$S_{ii'}$	$4 \times 10^{-3}$	0.0385	0.016	0.0335	0.0196	0	$5 \times 10^{-3}$	0.0694	0.013
$\Delta E^{\text{mod}}$	0	0.94	0.66	0.74	0.47	0	0	1.69	0.53
$\Delta E^{\text{calcd}}$	0	0.93	0.67	0.76	0.47	0	0	1.69	0.53

<sup>a</sup> HAM/3 data have been used for  $\pi$  levels and STO-3G data for  $n$  levels. Together with the coefficients of Table I, we have used  $K_n = -41.0$  eV,  $K_\pi = -24.3$  eV, and the experimental IE's of Table II.

MO's with ionization energies  $\alpha_i^+$  and  $\alpha_i^-$ , respectively) derives from the combination of only two isoenergetic MO's (one for each pyrimidine ring),  $\varphi_i \equiv \varphi_r$ , that are both doubly occupied and have ionization energies  $\alpha_i^0$ . In a first step the IE's of each subunit are perturbed (no direct coupling) by the field of the second fragment; this effect is, however, generally negligible (with the only exception being the destabilization of all the levels in I; vide infra), and hence, we will base our analysis on unperturbed  $\alpha_i^0$  values. On this basis, the IE's of each pair  $i$  of MO's in bipyrimidines are given by

$$\alpha_i^+ = \frac{\alpha_i^0 - \beta_{ii'}}{1 + S_{ii'}} \quad (1a)$$

$$\alpha_i^- = \frac{\alpha_i^0 + \beta_{ii'}}{1 - S_{ii'}} \quad (1b)$$

and the corresponding MO's are

$$\psi_i^+ = \frac{\varphi_i + \varphi_r}{[2(1 + S_{ii'})]^{1/2}} \quad (2a)$$

$$\psi_i^- = \frac{\varphi_i - \varphi_r}{[2(1 - S_{ii'})]^{1/2}} \quad (2b)$$

In the above equations,  $S_{ii'}$  is the overlap between the degenerate MO's  $\varphi_i$  and  $\varphi_r$  of the two pyrimidine rings and  $\beta_{ii'}$  is the corresponding coupling. We further assume that the coupling terms are proportional to the corresponding overlaps through factors  $K_n$  and  $K_\pi$ , which depend only on the symmetry ( $n$  or  $\pi$ ) of  $\varphi_i$ . Finally

$$\Delta E_i = \alpha_i^+ - \alpha_i^-$$

$$\Delta \alpha_i = \alpha_i^0 - [(\alpha_i^+ + \alpha_i^-)/2]$$

give the splitting and the destabilization of the barycenter with respect to  $\alpha_i^0$  for each pair of orbitals. Equation 1 shows the importance of the explicit consideration of the overlap because only in this case are the  $\Delta \alpha_i$  different from zero and, in agreement with experimental findings, negative.

The reliability of the proposed model can be judged by the results shown in Table VII. We note that for  $n_A$  levels only the use of STO-3G data gives similar splittings for I and IV. For  $\pi$  levels, on the contrary, HAM/3 and STO-3G data give very similar results.

In Table VII we have not reported the results for the non-symmetric molecule (III) and for the  $n_S$  levels of all the bipyrimidines. In fact, in these cases another effect contributes to the determination of the splittings between ionic states: if the percentage of nitrogen orbitals in the two MO's of a pair is different, the MO characterized by the larger contribution of the more electronegative nitrogen atoms is stabilized. The dissymmetry between MO's of the same pair derives from at least two effects: (i)  $\psi_i^+$  and  $\psi_i^-$  do not strictly derive only from  $\varphi_i$  but contain also small contributions from other MO's. This effect is particularly significant for  $n_S$  states, which are near in energy to other MO's of the same symmetry. (ii) In nonsymmetric bipyrimidines the reference states are not strictly degenerate due to different field effects. Both effects can be accounted for by more complicated models<sup>56-58</sup> that, however, do not add further significant novelties;

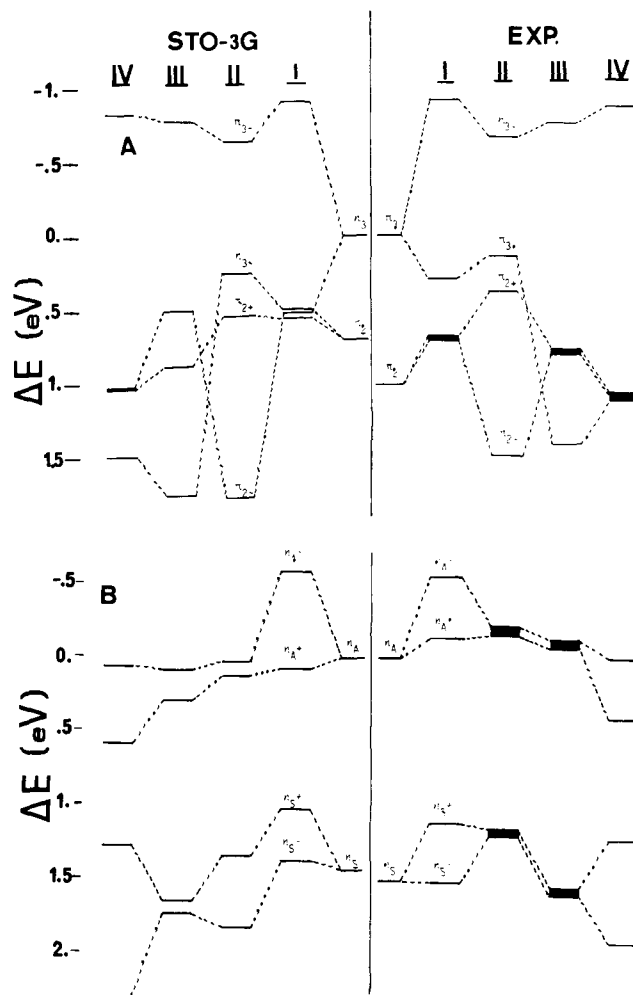


Figure 7. Comparison between STO-3G and experimental variations of energy levels in going from pyrimidine to different bipyrimidines: (A)  $\pi$  orbitals; (B)  $n$  orbitals. The  $\pi_3$  (A) and  $n_A$  (B) levels of pyrimidine are chosen as references (0.0 eV) for both the STO-3G and experimental data.

hence, we found it sufficient to use in the present context the simple two-orbital model previously described. On the other hand, electrostatic repulsions between nonbonded atoms can be conveniently added to the model. As a consequence, vicinal dispositions of atoms (belonging to different pyrimidine rings) bearing significant charges of the same sign result in an overall destabilizing effect. This explains the general destabilization of the ionic levels of I with respect to all the other bipyrimidines.

The above model is also able to explain the relative ordering of the first three ionic states in IV with respect to I. In fact, inspection of Table VII shows that the splittings of the pairs  $n_{A^+}$ ,  $n_{A^-}$  and  $\pi_{2^+}$ ,  $\pi_{2^-}$  are nearly the same in both molecules, while the splitting of the pair  $\pi_{3^-}$ ,  $\pi_{3^+}$  is much larger in IV. As a consequence, the greatly destabilized  $\pi_{3^-}$  level is found in IV at an

(56) Heilbronner, H.; Schmelzer, A. *Helv. Chim. Acta* **1975**, *58*, 936.

(57) Klessinger, M. *Theor. Chim. Acta* **1978**, *49*, 77.

(58) Barone, V.; Lej, F.; Russo, N. *J. Mol. Struct.* **1982**, *86*, 239.

intermediate position between  $n_{A^+}$  and  $n_{A^-}$  levels, and the  $\pi_{3+}$  level becomes more stable than the nearly degenerate  $\pi_{2-}$  and  $\pi_{2+}$  MO's.

Finally, we point out that in this simple model the splitting and the barycenter destabilization for each pair of MO's are dominated by the contributions of  $C_{ir}$  atoms (1-2 interactions), because already for 1-3 interactions the overlap (and hence the coupling) becomes an order of magnitude lower. The main exception is found for the  $n$  levels of (I): due to the strong localization of these orbitals on nitrogen atoms, 1-4 interactions between lone pairs are of the same order of magnitude as the 1-2 interactions between  $C_{ir}$  atoms. However, 1-3 interactions between  $C_{ir}$  and N atoms are antibonding (Scheme I) and nearly compensate (there are two 1-3 interactions for each 1-4 interaction) the direct coupling between lone pairs; as a consequence, even in this case, the splitting is determined by the  $C_{ir}$  atoms.

On this basis we can gain better insight into the splittings between  $n_{A^+}$  and  $n_{A^-}$  levels in the whole series of molecules. In fact, the coefficients of C2 and C5 atoms (which become  $C_{ir}$  atoms in I and IV, respectively) are similar in the  $n_A$  level of pyrimidine and much higher than the coefficient of the C4 atom (which becomes  $C_{ir}$  in II and III). As a consequence, we expect

$$\Delta E(I) \approx \Delta E(IV) > \Delta E(II) \approx \Delta E(III)$$

in perfect agreement with experimental findings.

Analogous considerations explain the behavior of  $\pi_2$  orbitals: they are nearly degenerate in I and IV because the participation of  $C_{ir}$  AO's is symmetry forbidden. The partial breakdown of symmetry constraints in II and III allows a contribution of  $C_{ir}$  atoms to these orbitals; it results in a significant splitting. Finally, in the  $\pi_3$  orbital of pyrimidine, the coefficient of the C5 atom is larger than the coefficient of the C2 atom (Table I); as a consequence, the splitting between  $\pi_{3+}$  and  $\pi_{3-}$  levels is larger in IV than in I.

### Concluding Remarks

From an experimental point of view, the relevant differences among spectral patterns of the four examined compounds, despite their structural similarity, point out large differences in the interactions between the two pyrimidine rings. In this frame, the HAM/3 method has been proven to be the most successful in

reproducing quantitatively absolute energy values and relative ordering of ionic states. Ab initio STO-3G computations can be profitably used to analyze the origin of trends and relative spacings (within the two groups of  $n$  and  $\pi$  orbitals) with reference to the pyrimidine fragment.

An analysis of the relative importance of the various effects in determining the relative ordering and splitting of ionic states has been performed also. It shows that 1-3 and 1-4 interactions are negligible or nearly compensate each other, so that the most relevant role is always played by the direct coupling between AO's of  $C_{ir}$  atoms and/or by the percentage of nitrogen AO's (due to their higher electronegativity).

On this basis, a simple interpretative model that leads to the following rules of thumb has been proposed: (1) The bigger the coefficients of atomic orbitals of  $C_{ir}$  are the larger is the splitting between a pair of levels (deriving from the same level of pyrimidine). (2) The barycenter of a pair of related orbitals is always destabilized with respect to the corresponding ionization energy of pyrimidine due to four-electron two-level interactions. (3) Due to electrostatic repulsion, vicinal dispositions of nitrogen lone pairs destabilize the resulting MO's.

The only effect that cannot be reproduced by the proposed model is the dissymmetry between MO's belonging to the same pair, which gives the last rule: (4) The higher the contribution of more electronegative atoms is, the larger the stabilization of the corresponding MO.

In conclusion, we think that a careful analysis of the interactions present in a related class of molecules may provide a valuable aid in the interpretation of PE spectra of large molecules in which first-principle computations are hardly feasible. Simple models based on well-chosen fragments and supported by HAM/3 computations seem particularly adequate in this connection.

**Acknowledgment.** We acknowledge Professor E. Lindholm for his useful comments and careful reading of the manuscript, Professor T. Kauffmann for the generous gift of samples of the different bipyrimidines, and Dr. L. Asbrink for providing a copy of the HAM/3 program.

**Registry No.** I, 34671-83-5; II, 2426-94-0; III, 28648-89-7; IV, 56598-46-0; pyrimidine, 289-95-2.

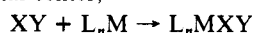
## Oxidative Addition of Hydrogen to Bis(phosphine)platinum(0) Complexes: An ab Initio Theoretical Treatment

J. Oakey Noell<sup>†</sup> and P. Jeffrey Hay\*

Contribution from the Theoretical Division, Los Alamos National Laboratory, University of California, Los Alamos, New Mexico 87545. Received June 8, 1981

**Abstract:** Ab initio molecular orbital methods utilizing relativistic core potentials and correlated wave functions are employed to examine the oxidative addition reactions  $H_2 + Pt(PH_3)_2 \rightarrow cis-Pt(PH_3)_2H_2$  and  $H_2 + Pt[P(CH_3)_3]_2 \rightarrow cis-Pt[P(CH_3)_3]_2H_2$ . For this symmetry-allowed process, an activation barrier of 17 kcal/mol and an exothermicity of 7 kcal/mol are calculated at the SCF level for the  $PH_3$  liquid; similar values are obtained for the  $P(CH_3)_3$  ligand. This implies a barrier of 24 kcal/mol for the reverse reductive elimination reaction. These values were not significantly altered in MC-SCF or CI calculations. This barrier is consistent with available data on the analogous process in six-coordinate complexes but is puzzling in light of the paucity of known four-coordinate cis dihydrides. The reaction is analyzed in terms of three phases: initial repulsion, partial transfer of charge from the platinum to the hydrogen, and final metal-hydrogen bond formation. The relative energies of the cis and trans isomers are also discussed.

The well-established inorganic reaction,<sup>1-4</sup> oxidative addition of ligands to a metal center,



has often been postulated in homogeneous catalytic cycles.<sup>5</sup> From a mechanistic viewpoint, these reactions have continued to be the

subject of many studies. For additions to square-planar  $d^8$  complexes, one generally finds concerted additions of homonuclear

(1) Collman, J. P. *Acc. Chem. Res.* **1968**, *1*, 136.

(2) Vaska, L. *Acc. Chem. Res.* **1968**, *1*, 335.

(3) Halpern, J. *Acc. Chem. Res.* **1970**, *3*, 386.

(4) Cotton, F. A.; Wilkinson, G. "Advanced Inorganic Chemistry", 3rd ed.; Interscience: New York, 1972; p 772.

(5) James, B. R. "Homogeneous Hydrogenation"; Wiley: New York, 1973.

<sup>†</sup> Present address: Division 8343, Sandia National Laboratory, Livermore, CA 94550.